DEVELOPMENT OF A MODEL - BASED IMPEDANCE CONTROLLER FOR ELECTROHYDRAULIC SERVOS

Ioannis Davliakos, Panagiotis Chatzakos and Evangelos Papadopoulos
Department of Mechanical Engineering, National Technical University of Athens
Heroon Polytechniou 9, 15780 Zografou, Athens, Greece
gdavliak@central.ntua.gr, pchatzak@central.ntua.gr, egpapado@central.ntua.gr,

ABSTRACT
In this paper, a model-based impedance controller for electrohydraulic servosystems is developed. Rigid body and electrohydraulic models, including servovalve models are employed and described by a set of integrated system equations. Friction and leakage of hydraulic elements are also included. The control law consists of two signals, a feedback and a feedforward signal. An impedance filter modifies a desired trajectory according to a specified behaviour. The modified trajectory is fed to a simplified system model to reduce the effects of the nonlinear hydraulic dynamics. An example one degree of freedom servomechanism is studied. Simulations with typical desired trajectories are presented and a good performance of the controller is obtained.

KEY WORDS
Electrohydraulic Servosystems, Impedance, Force Control

1. Introduction

The combination of hydraulics science with servo control, or *hydrotronics*, has given new thrust to hydraulics applications, [1]. The main reasons why hydrotronics are preferred to electromechanical drives in some industrial and mobile applications, include their ability to produce large forces at high speeds, their high durability and stiffness, and their rapid response, [2].

Control techniques are used to compensate for the nonlinearities of electrohydraulic servosystems. Nonlinear adaptive control techniques for hydraulic servosystems have been proposed by researchers assuming linearization [3] and backstepping [4], approaches. A robust force controller design based on the nonlinear Quantitative Feedback Theory, has been implemented on an industrial hydraulic actuator, taking into account system and environmental uncertainties, [5].

Hydraulic systems differ from electromechanical ones, in that the force or torque output is not proportional to actuator current and therefore, hydraulic actuators cannot be modeled as force/ torque sources. As a result, controllers that have been designed for robot control, assuming the capability of setting actuator force/ torque, cannot be used here. To use such controllers, a hydraulic actuator must be able to apply a desired force.

A unified approach to the control of a manipulator applicable to free motions, kinematically constrained motions, and dynamic interaction between the manipulator and its environment has been examined in [6]. Techniques for implementing a desired manipulator impedance and for choosing the impedance appropriate to a given application using optimization theory were presented, [6].

A model-based, feedforward-feedback impedance controller of hydraulic servosystems for high-performance hydraulic joints [7] has been proposed, in which an impedance filter adjusts the desired trajectory according to a prescribed behaviour in free space and in contact. Similar work has been presented in [8], where a position-based impedance controller for an industrial hydraulic manipulator is developed. Further, impedance controllers have been studied and implemented on teleoperated hydraulic servosystems for heavy duty works, [9], [10].

In this paper, a model-based impedance controller for electrohydraulic servosystems is developed. Dynamic models are presented that describe the rigid body equations of motion and the hydraulic dynamics. Friction and leakages of hydraulic elements are included in the model. The control law includes two control signals, a feedback and a feedforward one. An impedance filter modifies a desired trajectory according to a specified behaviour. The modified trajectory is fed to a simplified model in order to reduce the effects of the nonlinear hydraulic dynamics. A case study of a servo-mechanism with one degree of freedom is studied in detail. Results show that a good performance of the controller is obtained. The approach can be further extended to hydraulic manipulator and simulator control.

2. Elements of Electrohydraulic Servosystem Dynamic Modeling

In this section, the dynamic modeling of high performance electrohydraulic servocylinders is presented briefly. An electrohydraulic servosystem consists of a

servomechanism, including a servovalve, a servoactuator, a controller, a mechanical load and a hydraulic power supply. Next, simple models of major components are described.

An ideal single rod hydraulic cylinder is described by

$$Q_r = A_r \dot{x}_p \,, \quad r = 1, 2 \tag{1a}$$

$$p_1 A_1 - p_2 A_2 = F_p \tag{1b}$$

where Q_r are the flows through its two chamber ports, p_1, p_2 are the chamber pressures, A_1 is the piston side area, A_2 is the rod side area, x_p is the piston displacement and F_p is the piston output force. A real cylinder model also includes chamber oil compressibility, friction and other effects. However, these can be neglected at an initial stage.

A typical hydraulic servovalve consists of four symmetric and matched servovalve orifices making up a four-legged flow path of four nonlinear resistors, modulated by the input voltage. Thereby, the servovalve is modeled as the hydraulic equivalent of a Wheatstone bridge, see Fig. 1. When flow passes through the orifices 1 and 3 (path $P \to A \to B \to T$), flow leakages exist in the valve orifices 2 and 4. Respectively, when flow passes through the path $P \to B \to A \to T$, flow leakages exist in the valve orifices 1 and 3. This model is described by

$$Q_{v1} = f_1(i)\sqrt{p_s - p_1}, \quad Q_{v3} = g_1(i)\sqrt{p_2 - p_T} \tag{2a}$$

$$Q_{v2} = f_2(i)\sqrt{p_s - p_2}, \quad Q_{v4} = g_2(i)\sqrt{p_1 - p_T} \tag{2b}$$

where p_s and p_T are the power supply and return pressure of the servosystem, respectively, i is the servovalve motor current (control command), $f_1(i)$, $f_2(i)$, $g_1(i)$ and $g_2(i)$ are servovalve nonlinear orifice conductances, functions of the servovalve motor current. Because of servovalve symmetry, the following equations hold,

$$f_1(i) = g_1(i) = f_2(-i) \tag{3a}$$

$$f_2(i) = g_2(i) = f_1(-i) \tag{3b}$$

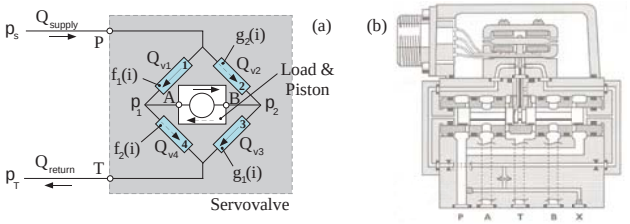

Fig. 1. a. Schematic model of servovalve. b. A drawing of a real servovalve.

In the case of an ideal hydraulic cylinder with a double rod, the two areas A_1 and A_2 are equal and therefore, (1) is simplified further.

Hydraulic equations must be appended with rigid body equations of motion that provide a relation between actuator torques/forces and the resulting accelerations. These are given by,

$$\mathbf{M}(\boldsymbol{q})\ddot{\boldsymbol{q}} + \boldsymbol{V}(\boldsymbol{q}, \dot{\boldsymbol{q}}) + \boldsymbol{G}(\boldsymbol{q}) + \boldsymbol{F}_{fr}(\dot{\boldsymbol{q}}) = \boldsymbol{\tau} \tag{4}$$

where $\boldsymbol{q}$ is the $n \times 1$ vector of generalized coordinates, $\mathbf{M}(\boldsymbol{q})$ is the $n \times n$ positive definite mass matrix, the $n \times 1$ vector $\boldsymbol{V}(\boldsymbol{q}, \dot{\boldsymbol{q}})$ represents forces/torques arising from centrifugal and Coriolis forces, the $n \times 1$ vector $\boldsymbol{G}(\boldsymbol{q})$ represents torques due to gravity, $\boldsymbol{F}_{fr}(\dot{\boldsymbol{q}})$ is the $n \times 1$ vector of the forces / torques due to friction and $\boldsymbol{\tau}$ is the $n \times 1$ vector of actuator joint torques.

A number of methods exists, that model the friction vector $\boldsymbol{F}_{fr}(\dot{\boldsymbol{q}})$, [12]. A widely used method suggests,

$$\boldsymbol{F}_{fr}(\dot{\boldsymbol{q}}) = \boldsymbol{F}_v(\dot{\boldsymbol{q}}) + \boldsymbol{F}_c(\dot{\boldsymbol{q}}) + \boldsymbol{F}_s \tag{5}$$

where $\boldsymbol{F}_v(\dot{\boldsymbol{q}})$, $\boldsymbol{F}_c(\dot{\boldsymbol{q}})$ and $\boldsymbol{F}_s$ are the viscous, Coulomb and static friction vector respectively.

The hydraulic and load dynamic response can be described by integrated system equations derived using a systems approach, such as the Linear Graph, [13], or Bond Graph methods, [14]. This approach leads to a set of nonlinear state space equations, the solution of which determines the system variables. To integrate these models to the mechanical load dynamics, one needs to provide expressions transforming pressure differences to forces, see (1b), and velocities to flows, see (1a). In general, hydraulic and load dynamics are described by nonlinear equations, of the form,

$$\begin{aligned} \dot{\boldsymbol{x}} &= \boldsymbol{f}(\boldsymbol{x}) + \boldsymbol{g}(\boldsymbol{x})\boldsymbol{u} \\ \boldsymbol{y} &= \boldsymbol{h}(\boldsymbol{x}), \qquad \boldsymbol{x_0} = \boldsymbol{x}(t_0) = \boldsymbol{x}(0) \end{aligned} \tag{6}$$

where $\boldsymbol{x}$ is a state column vector, $\boldsymbol{x_0}$ is the initial state column vector for initial time $t_0 = 0$, $\boldsymbol{u}$ is the input column vector, $\boldsymbol{y}$ is the output column vector and $\boldsymbol{f}(\boldsymbol{x})$, $\boldsymbol{g}(\boldsymbol{x})$, and $\boldsymbol{h}(\boldsymbol{x})$ are nonlinear functions.

3. Example: Modeling of a 1-DOF Servo

In this section, the dynamic model of a one-degree-of-freedom electrohydraulic servomechanism is developed. This servo is to be used as an actuator in a robotic Stewart type mechanism, [15], for 6-dof CNC machining, i.e. a six dof closed kinematic chain mechanism consisting of a fixed base and a movable platform with six linear actuators supporting it. The one dof mechanism is illustrated schematically in Fig. 2. Also, a typical view of a 6-dof Stewart platform is depicted in the same figure.

The angles of inclination of the actuator θ, and the

load φ shown in Fig. 2, can be expressed as function of the displacement of the actuator, x_p. The equation of motion for the complete system including actuator, load and beam, is derived applying the Lagrange formulation given by (4), which is written as

$$M(x_p)\,\ddot{x}_p + V(x_p, \dot{x}_p) + G(x_p) + F_{fr}(\dot{x}_p) = F_p \tag{7}$$

where $M(x_p)$ is a positive function, which represents the variable apparent mass of all moving masses including the piston mass, as seen by the actuator, $V(x_p, \dot{x}_p)$ contains the Coriolis and centrifugal terms, $G(x_p)$ represents the gravity term, F_p is the hydraulic force, which is applied by the piston and $F_{fr}(\dot{x}_p)$ is the friction term, which is described by (5) and is given by

$$F_{fr}(\dot{x}_p) = b\dot{x}_p + F_{c0}\,sign(\dot{x}_p) + F_s \tag{8}$$

where b is the parameter for viscous friction, F_{c0} is the parameter for Coulomb friction, and F_s is the static friction, which is given by

$$F_s = \begin{cases} F_{ext}, & |F_{ext}| < F_{s0},\ \dot{x}_p = 0,\ \ddot{x}_p = 0 \\ F_{s0}\,sign(F_{ext}), & |F_{ext}| > F_{s0},\ \dot{x}_p = 0,\ \ddot{x}_p \neq 0 \end{cases} \tag{9}$$

In (7), $M(x_p)$, $V(x_p, \dot{x}_p)$ and $G(x_p)$ are given by

$$M(x_p) = m_p + (4I_A l^4 + I_B L_1^2)\cdot(L_2 L_3 l^2)^{-1} \tag{10a}$$

$$V(x_p, \dot{x}_p) = [4l^2 L_4 (I_B r_1^2 + I_A l^2) - I_B L_3 L_2 L_1^2]\cdot(L_2^2 L_3^2 l^3)^{-1} \tag{10b}$$

$$G(x_p) = g\cdot[2L_3 L_2 l r_1 m_p + 2(r_1 + r_2) l^3 L_5 (2m + m_b) - r_1 L_4 (2m_p l + l_{cyl} m_{cyl} - m_p l_p)]\cdot(4r_1 r_3 l^2 \sqrt{L_3 L_2})^{-1} \tag{10c}$$

where r_1, r_2 and r_3 are defined in Fig. 2, m, m_b, m_p and m_{cyl} are the load, beam, piston, and cylinder masses respectively, I_A is the load and the load supportive beam moment of inertia about the rotation point A, I_B is a linear function of x_p and represents the cylinder and piston moment of inertia about the rotation point B, and l, L_1, L_2, L_3, L_4 and L_5 are expressed as functions of the displacement of the actuator, x_p,

$$l = l(x_p) \equiv l_{cyl} + x_p \tag{11a}$$

$$L_1 = L_1(x_p) \equiv l^2 + r_1^2 - r_3^2 \tag{11b}$$

$$L_2 = L_2(x_p) \equiv (r_1 + r_3)^2 - l^2 \tag{11c}$$

$$L_3 = L_3(x_p) \equiv l^2 - (r_1 - r_3)^2 \tag{11d}$$

$$L_4 = L_4(x_p) \equiv l^4 - (r_1^2 - r_3^2)^2 \tag{11e}$$

$$L_5 = L_5(x_p) \equiv r_1^2 + r_3^2 - l^2 \tag{11f}$$

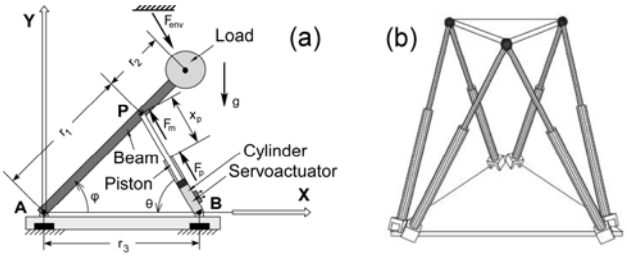

Fig. 2. a. Schematic view of the one DOF servomechanism model.
b. Schematic view of a six-dof Stewart Platform.

The hydraulics equations of the servomechanism are described by (1)-(3). One of the most important characteristics is the servovalve characteristic, $Q_v - \Delta p_v$. The flow through the cylinder and the piston output force applied to the load are given by (1a) and (1b) correspondingly. The pressure drop at the servovalve is expressed using (2), neglecting auxiliary elements pressure drops.

The application of continuity and compatibility laws, along with individual elements equations, leads to a set of eight nonlinear first order differential equations, in the form of (6), as follows,

$$\dot{p}_1 = [Q_{I,l1} - Q_{v2} - Q_{v4} - C_{p,in}(p_1 - p_2) - A_1 v_p] C_1^{-1} \tag{12a}$$

$$\dot{p}_2 = [Q_{v2} + Q_{v4} - Q_{I,l2} + C_{p,in}(p_1 - p_2) + A_2 v_p] C_2^{-1} \tag{12b}$$

$$\dot{p}_{C,l1} = [(p_s - p_{C,l1})/R_{l1} - Q_{I,l1}] C_{l1}^{-1} \tag{12c}$$

$$\dot{p}_{C,l2} = [Q_{I,l2} - (p_{C,l2} - p_T)/R_{l2}] C_{l2}^{-1} \tag{12d}$$

$$\dot{Q}_{I,l1} = [p_{C,l1} - p_1 - C_{R1} Q_{v1} |Q_{v1}|] I_{l1}^{-1} \tag{12e}$$

$$\dot{Q}_{I,l2} = [p_2 - p_{C,l2} - C_{R3} Q_{v3} |Q_{v3}|] I_{l2}^{-1} \tag{12f}$$

$$\dot{v}_p = M^{-1}(x_p)[A_1 p_1 - A_2 p_2 - V(x_p, \dot{x}_p) - G(x_p) - F_{fr}(\dot{x}_p)] \tag{12g}$$

$$\dot{x}_p = v_p \tag{12h}$$

where $Q_{I,l1}$, $Q_{I,l2}$ are the flows in hydraulic power and return line correspondingly, $p_{C,l1}$, $p_{C,l2}$ are respectively the pressures of hydraulic power and return line regarding with the lines' capacitances, I_{l1}, R_{l1}, and C_{l1} are the inertance, resistance and capacitance of hydraulic power line respectively, I_{l2}, R_{l2}, and C_{l2} are the inertance, resistance and capacitance of hydraulic return line respectively, C_1, and C_2 are the fluid capacitance in the servoactuator chambers, and $C_{p,in}$ is the internal leakage coefficient of piston.

The force acting on the load and beam, see Fig. 2, is given by

$$F_m = M_m(x_p)\,\ddot{x}_p + V_m(x_p, \dot{x}_p) + G_m(x_p) \tag{13}$$

where $M_m(x_p)$ is the part of $M(x_p)$ which represents the variable apparent mass of the load and beam, $V_m(x_p, \dot{x}_p)$ is the part of $V(x_p, \dot{x}_p)$, which contains velocity terms, and $G_m(x_p)$ is the part of $G(x_p)$ which represents gravity terms of the load mass and beam.

4. Control Design

Impedance control essentially allows a physical system to emulate another simpler one assuming the new behaviour is within the capabilities of the physical system. In this section a model-based impedance control design for electrohydraulic servosystems is developed. This law is applied to the examined single dof application. The control design strategy presented here involves two control parts, a feedback and a feedforward one.

Feedback Control Scheme: In the model-based impedance approach, a new desired trajectory is computed and is called an impedance filter. The design of this new trajectory includes a set of impedance parameters, which are responsible for the good behaviour of the tracking performance.

A typical response system behaviour is given by a second order system, [6]. The desired behaviour can be extended considering the virtual point position as a time function and including the velocity, acceleration and force error in the control law scheme, in general. The impedance filter approach used for the electrohydraulic servomechanism at hand, is described by

$$M_d(\ddot{x}_e - \ddot{x}_{p,des}) + B_d(\dot{x}_e - \dot{x}_{p,des}) + K_d(x_e - x_{p,des}) = F_{env} \quad (14)$$

where M_d, B_d, K_d are respectively the desired inertia, damping and stiffness (desired impedance parameters) describing the desired second order behaviour, x_e is the new desired impedance trajectory, which depends on the desired one, $x_{p,des}$, and the contact force, $x_{p,des}$ is the desired trajectory of the system and F_{env} is the environment force acting to the system, which can be measured by a force sensor and can be approximated by,

$$F_{env} = K_{env}(x_{env} - x_p) \quad (15)$$

where K_{env} is a positive constant which symbolizes the environment stiffness and x_{env} is a virtual point of the environment.

The model-based impedance control law is introduced by the feedback valve current, i_{fb}. This loop can include a number of terms depending on the robustness and performance required. Examples include the following feedback laws,

$$i_{fb} = K_v(\dot{x}_e - \dot{x}_p) + K_p(x_e - x_p) \quad (16a)$$

$$i_{fb} = K_v(\dot{x}_e - \dot{x}_p) + K_p(x_e - x_p) + K_f(F_{e,des} - F_e) \quad (16b)$$

where x_e is determined by (14), K_p, K_v and K_f are control gains, F_e is found subtracting environmental force from force acting on the load mass and beam and $F_{e,des}$ is the impedance desirable force acting on the load mass and beam. The forces F_e and $F_{e,des}$ are given respectively by

$$F_e = F_m - F_{env} \quad (17a)$$

$$F_{e,des} = M_m(x_e)\,\ddot{x}_e + V_m(x_e, \dot{x}_e) + G_m(x_e) \quad (17b)$$

Here, the control law given by (16b) is studied. The impedance control law is examined taking into account the servovalve orifice conductances are assumed to be linear functions of the input current. Therefore, the flows through the orifices of the servovalve are written as

$$Q_{v1} = (K_1 i + K_{0,1})\sqrt{p_s - p_1},\ Q_{v3} = (K_1 i + K_{0,1})\sqrt{p_2 - p_T} \quad (18a)$$

$$Q_{v2} = (K_2 i + K_{0,2})\sqrt{p_s - p_2},\ Q_{v4} = (K_2 i + K_{0,2})\sqrt{p_1 - p_T} \quad (18b)$$

where i is the valve current, K_1, $K_{0,1}$, K_2 and $K_{0,2}$ are positive constants, which correspond to the main and leakage valve flow path.

Feedforward Control Scheme: A feedforward control signal can be added in the control scheme to further reduce deviations from the desired trajectory. This current must be determined such that the physical plant behaves like the desired system in noncontact and contact regimes. Schematically, the proposed control scheme is depicted in Fig. 3.

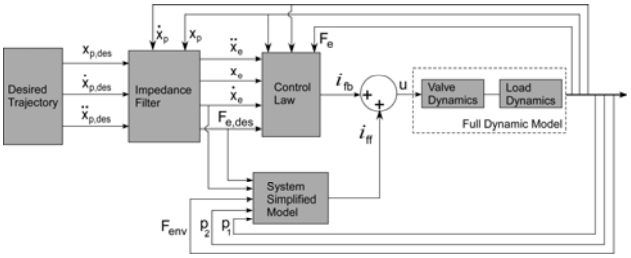

Fig. 3. Schematic view of the full model-based impedance controller diagram.

The feedforward input current is determined using a simplified model of the hydraulic servosystem. The use of a simplified model in the feedforward loop yields practically the same response as that using the full model. Moreover, the main advantage of this approach is a significant decrease in the computational burden required for simulation. Indeed, neglecting the internal leakage coefficient of piston and the servovalve leakages, (12a-b) are written as

$$\dot{p}_1 = [Q_{v1} - A_1 v_p] C_1^{-1} \quad (19a)$$

$$\dot{p}_2 = [A_2 v_p - Q_{v3}] C_2^{-1} \quad (19b)$$

Further, the continuity equation to each of the piston chambers, [11], and the combination of (19a-b) yields

$$V_t(4\beta_e)^{-1}\Delta\dot{p}_L = Q_L - (A_1 - A_2)v_p \tag{20}$$

where V_t is the total volume of fluid under compression in both chambers, β_e is the effective bulk modulus of the fluid, $\Delta p_L = p_1 - p_2$ is the piston pressure drop and Q_L is the load flow, which is given by, [11]

$$Q_L = F(i)\sqrt{(p_s - sign(i)\Delta p_L)/2} \tag{21}$$

where

$$F(i) = \begin{cases} f_1(i) = K_1 i + K_{0,1}, & i > 0 \\ f_2(i) = K_2 i + K_{0,2}, & i < 0 \end{cases} \tag{22}$$

Using (18)-(22), the feedforward current is determined. For instance, when $i > 0$ the current is given by

$$i_{ff} = \frac{V_t(4\beta_e)^{-1}\Delta\dot{p}_L + (A_1 - A_2)v_p}{K_1\sqrt{(p_s - sign(i)\Delta p_L)/2}} - \frac{K_{0,1}}{K_1} \tag{23}$$

Finally, the full control law scheme of the servosystem is given by the total valve current of the feedback and feedforward current,

$$i_t = i_{fb} + i_{ff} \tag{24}$$

Substituting (24) to state equations (12), taking into account (14), (16) – (18) and associating appropriate (12), is resulted

$$\ddot{e}_e + K_{v,e}\dot{e}_e + K_{p,e}e_e = 0 \tag{25}$$

where $e_e = x_e - x_p$ and $K_{v,e}, K_{p,e}$ are positive quantities, which represent the control gains. Last equation represents the system error dynamics and proves that the system is stable.

A custom-designed benchmark setup, shown in Fig. 4, was built at the NTUA to test the proposed controller. The particular design of the setup allows for easy changes in the static and dynamic components of the inertial load, driven by the actuator. This is achieved by varying the angle of the cylinder with respect to the horizontal, and by adding or removing loads.

A Moog G122-202A1 Series controller is used. To read servocylinder headside and rodside pressure, pressure sensors on the valve manifold are used. The piston rod position is read by a built-in analog LDT. A force cell at the end of the rod provides the force transmitted to the load. To use nonlinear and model based controllers, the PID control section of the card is bypassed and the card is used only for reading feedback measurements and for sending the appropriate control voltages to the servoamplifier. The servoamplifier in turn sends appropriate currents to the servovalve.

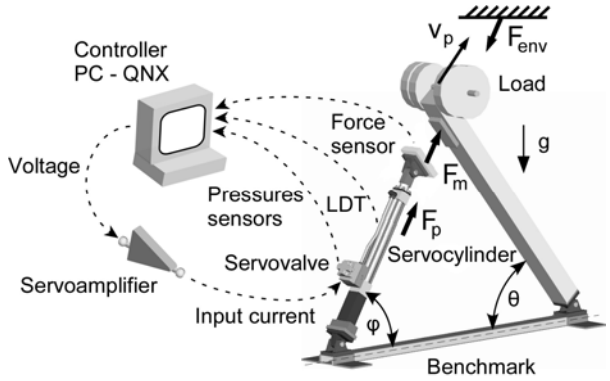

Fig. 4. Schematic of control system setup and benchmark.

5. Simulation Results

The tracking performance of the controller is evaluated on the full hydraulic servosystem, described by (12a-h), using Matlab/Simulink. System parameters include the load supportive beam mass and inertia, $m_b = 15.11\,\text{kg}$, $I_b = 6.32\,\text{kgm}^2$ and geometrical parameters such as $r_1 = 1.04\,\text{m}$, $r_2 = 0.08\,\text{m}$ and $r_3 = 1.64\,\text{m}$, see Fig. 2. Friction parameters are $b = 200$ Ns/m, $F_{c0} = 50$ N, $F_{s0} = 20$ N.

Simulations runs were obtained using a number of desirable trajectories. As an example, Fig. 5 shows typical results with $m = 60\,\text{kg}, K_p = 10^3\,A/m, K_v = 3\times10^{-4}\,As/m$ $K_f = 2\times10^{-6}\,A/N$ and $K_{env} = 5\times10^4\ N/m$. A stiff wall is present at $x_{env} = 0.045\,m$. A desired impedance parameters selection of the system response are $K_d = 10\,N/m$, $B_d = 20\,Ns/m$ and $M_d = 0.1kg$, [7]. Finally, the natural frequency is determined as $\omega_n = \sqrt{K_d/M_d} = 10\,rad/s$. The piston displacement and velocity responses, the input signal, the environment force response, as well as the load power and chamber pressures histories are shown in Fig. 5.

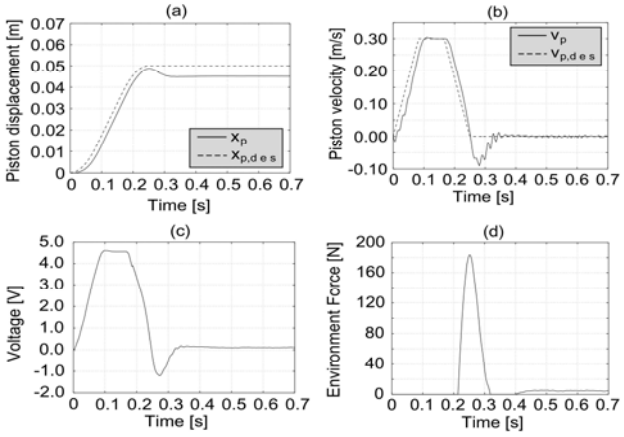

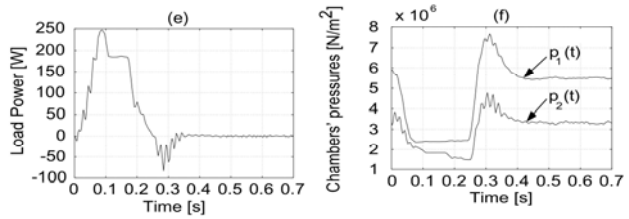

Fig. 5. Simulation results. (a) Piston displacement response, (b) Piston velocity response, (c) Input signal, (d) Environment force response, (e) Load power history, (f) Chamber pressures histories.

The robustness of the controller can be demonstrated by applying the controller to the system in the case of erroneous parameter estimation. For example, assume that the load, cylinder mass, beam mass, cylinder length and r_2 are estimated to be 5% larger than their true values, while the piston mass, piston length, r_1 and r_3 are estimated to be 5% smaller. In this case, despite these errors, the controller leads the system to the desired conditions, albeit with some intermediate oscillation, as can be seen from the piston displacement and velocity responses, shown in Fig. 6.

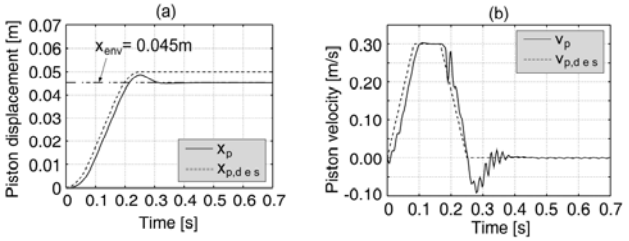

Fig. 6. Simulation results with parameter estimation error. (a) Piston displacement response, (b) Piston velocity response.

6. Conclusions

A model based impedance controller was developed for electrohydraulic servosystems, using a position-based impedance scheme. The control law included two control signals, a feedback and a feedforward one. Full rigid body and electrohydraulic models, including servovalve models were employed and described by a set of integrated system equations. The proposed methodology was illustrated by a detailed example. Simulations with typical desired trajectories were presented and a good performance of the controller was obtained. The approach can be further extended to hydraulic manipulator and simulator control.

5. Acknowledgements

Support by the EPAN Cooperation Program 4.3.6.1.b (Greece-USA 035) of the Hellenic General Secretariat for Research and Technology and the NTUA Senator Committee of Basic Research Programme "Protagoras", R.C. No. 10, is acknowledged.

References:

[1] K. Six, T. A. Lasky, & B. Ravani, A Time-Delayed Dynamic Inversion Scheme for Mechatronic Control of Hydraulic Systems. *IEEE/ASME Int. Conf. on Advanced Intelligent Mechatronics Proc.*, Como, Italy, 2001, 1232–1238.

[2] M. Jelali, & A. Kroll, *Hydraulic Servosystems. Modelling, Identification and Control* (Springer, 2003).

[3] D. Garagic, & K. Srinivasan, Application of Nonlinear Adaptive Control Techniques to an Electrohydraulic Velocity Servo-mechanism. *IEEE Trans. on Control Systems Tech.*, *12*(2), 2004, 303–314.

[4] M. R. Sirouspour, & S. E. Salcudean, Nonlinear Control of Hydraulic Robots. *IEEE Trans. on Robotics and Automation*, *17*(2), 2001, 173–182.

[5] N. Niksefat, & N. Sepehri, Robust Force Controller Design for an Electro-Hydraulic Actuator Based on Nonlinear Model. *Proc. 1999 IEEE Int. Conf. Robotics & Automation*, San Francisco, 200–206.

[6] N. Hogan, Impedance Control: An approach to manipulation: Part I – Theory, Part II – Implementation, Part III – Applications. *ASME Journal of Dynamic Systems, Measurement and Control, 107*, March 1985, 1-24.

[7] G. Bilodeau, & E. Papadopoulos, A Model-Based Impedance Control Scheme for High-Performance Hydraulic Joints. *Proc. 1998 Int. Conf. on Intelligent on Robotics & Applications*, Santa Barbara, CA, October 1998.

[8] B. Heinrichs, N. Sepehri, & A.B. Thornton-Trump, Position-Based Impedance Control of an Industrial Hydraulic Manipulator. *IEEE Control Systems*, February 1997, 46-52.

[9] S. Tafazoli, S. E. Salcudean, K. H. Zaad, & P.D. Lawrence, Impedance Control of a Teleoperated Excavator. *IEEE Trans. on Control Systems Tech.*, *10*(3), 2002, 355–367.

[10] Q.P. Ha, Q.H. Nguyen, D.C. Rye, & H.F. Durrant-Whyte, Impedance Control of a hydraulically actuated robotic excavator. *Automation in Construction 9*, 2000, 421-435.

[11] H. E. Merritt, *Hydraulic Control Systems* (J. Wiley, 1967).

[12] B.A. Helouvry, P. Dupont, & C.C. De Wit, A Survey of Models, Analysis Tools and Compensation Methods for the Control of Machines with Friction. *Automatica*, *30*(7), 1994, 1083-1138.

[13] E. Papadopoulos, & Y. Gonthier, On the Development of a Real-Time Simulator Engine for a Hydraulic Forestry Machine. *Int. Journal of Fluid Power*, *3*(1), 2002, 55-65.

[14] R. Rosenberg, & D. Karnopp, *Introduction to Physical System Dynamics* (McGraw Hill, New York, NY, 1983).

[15] D. Stewart, A platform with six degrees of freedom. *Proc. of the IMechE*, *180*(15), Pt. 1, 1965-66, 371-385.